

Graph Theory Based $N - 1$ Transmission Contingency Selection and Its Application in Security-constrained Unit Commitment

Lu Nan, Yikui Liu, Lei Wu, Tianqi Liu, and Chuan He

Abstract—Contingency analysis is an important building block in the stability and reliability analysis of power grid operations. However, due to the large number of transmission lines, in practice only a limited number of contingencies could be evaluated. This paper proposes a graph theory based $N - 1$ contingency selection method to effectively identify the most critical contingencies, which can be used in security-constrained unit commitment (SCUC) problems to derive secure and economic operation decisions of the power grid. Specifically, the power flow transferring path identification algorithm and the vulnerability index are put forward to rank individual contingencies according to potential transmission line overloads. Effectiveness of the proposed $N - 1$ contingency selection method is quantified by applying the corresponding SCUC solution to the full $N - 1$ security evaluation, i.e., quantifying total post-contingency generation-load imbalance in all $N - 1$ contingencies. Numerical results on several benchmark IEEE systems, including 5-bus, 24-bus, and 118-bus systems, show effectiveness of the proposed method. Compared with existing contingency selection methods which usually resort to full power flow calculations, the proposed method relies on power grid topology to effectively identify critical contingencies for facilitating the optimal scheduling of SCUC problems.

Index Terms—Concentric relaxation, contingency analysis, graph theory, security-constrained unit commitment (SCUC), shortest path, vulnerability index.

I. INTRODUCTION

WHILE the continued expansion of transmission capacities and the enhancement of power grid interconnections could contribute to improving power system stability and reliability, they also increase topological complexity. Indeed, in a sophisticated networked power grid, unexpected outages of elements such as generators and/or transmission lines, would challenge system operation security, resulting in

supply-demand imbalances and even large-area blackouts.

Consequently, $N - 1$ contingency analysis has been widely implemented in industry practice to ensure system operation security against any single element failure. However, an exhaustive contingency analysis would force a heavy computational burden, especially for large-scale power grids. Specifically, in security-constrained unit commitment (SCUC) problems, computation time could grow dramatically with the increase in the number of contingencies. Indeed, computational performance of many other related power system applications [1], [2] such as transmission switching, also highly relies on the number of contingencies considered to guarantee secure operation of the system. This motivates the study on identifying the most critical contingencies without full power flow calculation, which can be efficiently incorporated in the constraints of SCUC model to access operational security of power systems. Generally, $N - 1$ contingency analysis includes two steps of contingency selection and contingency evaluation [3], in which the former selects a set of most critical contingencies that could potentially threaten operational security of power systems while the latter examines severity of the selected contingency sets.

Existing research mainly focused on two types of methods in contingency selection: power flow based methods [4]-[12] and performance index (PI) based methods [13]-[18].

1) Power flow based methods. The power flow based methods often use information on power grid topology, load, generation, as well as operation mechanisms. References [4] and [5] discussed power flow based transmission contingency analysis methods while focusing on acceleration approaches to improve computational efficiency. Reference [5] further demonstrated that computation time and solution quality would highly rely on the number of iterations of power flow calculation. Reference [6] developed a real-time contingency analysis package with transmission switching using AC power flow to evaluate potential violations of critical contingencies. Reference [7] used nodal parallel computation to achieve fast contingency screening. Reference [8] established a transient heat balance based power flow model to select contingencies while considering transient thermal behaviour of transmission lines. Reference [9] proposed a contingency selection and ranking method, in which contingencies were simulated and ranked via a probabilistic PI. Reference [10] proposed an $N - 1 - 1$ contingency selection and ranking

Manuscript received: August 31, 2019; accepted: March 13, 2020. Date of CrossCheck: March 13, 2020. Date of online publication: August 10, 2020.

This article is distributed under the terms of the Creative Commons Attribution 4.0 International License (<http://creativecommons.org/licenses/by/4.0/>).

L. Nan, T. Liu, and C. He are with the College of Electrical Engineering, Sichuan University, Chengdu, China, and L. Nan is also with the Department of Electrical and Computer Engineering, Stevens Institute of Technology, Hoboken, NJ 07901, USA (e-mail: lnan1@stevens.edu; tqliu@scu.edu.cn; he_chuan@scu.edu.cn).

Y. Liu and L. Wu (corresponding author) are with the Department of Electrical and Computer Engineering, Stevens Institute of Technology, Hoboken, NJ 07901, USA (e-mail: yliu262@stevens.edu; lei.wu@stevens.edu).

DOI: 10.35833/MPCE.2019.000602



method, in which AC power flows for all $N-1$ contingencies were calculated and AC line outage distribution factors (LODFs) were further derived to screen candidate lines and construct $N-1-1$ contingency lists. However, multiple candidate contingencies could have the same LODF value and thus were unable to be ranked.

Indeed, although AC power flow methods [4]-[10] could improve the accuracy and credibility of contingency selection, their heavy computational burden prevents the direct adoption in many time-restricted applications. Alternatively, the DC power flow method is applied to contingency selection because of their computational advantages. Reference [11] presented two contingency screening methods for $N-2$ outages, in which the first method used LODF only and the second method further considered actual power flows and capacity limits of individual lines. However, the performance in terms of contingency list size and computational complexity highly depends on a prespecified threshold. Reference [12] proposed an $N-2$ contingency selection method that guaranteed zero-missing rate in DC approximation models, as well as a safety certificate concept to accelerate the contingency screening process. However, the methods in [11] and [12] were unable to identify critical $N-2$ contingencies that caused system islanding.

2) PI based methods. Two categories of PIs have been widely used for contingency selection because of their computational advantages: operative indices based on static or transient states of power systems [13]-[14], and topological structure indices based on complex network theory [15]-[18]. Operative indices often use information on operation mechanisms, while topological structure indices only use power grid topological structure. In the first category, [13] proposed a risk index to rank and select contingencies by considering occurrence probabilities and the corresponding consequences. Reference [14] proposed a severity index to rank $N-1$ voltage contingencies through a combination of a linear sensitivity evaluation with respect to voltages and an eigenvalue analysis, with which contingencies resulting in system islanding could be identified. In the second category, indices based on the concepts in complex network theory such as average path length [15], betweenness [16], centrality [17], and degree [18], were studied. However, contingency lists created via simple PIs were recognized as inaccurate [19], while advanced PIs presenting better accuracy might lose advantages in computational performance [20].

It can be observed that existing contingency selection methods are faced with a trade-off between high accuracy and heavy computational burdens, which is of importance for many power system applications that are time-restricted and need to be security-guaranteed. One of the most important applications is to solve the SCUC problem. Specifically, in the SCUC problem, security constraints are generated referring to the contingency list that contains a limited number of representative contingencies. An inaccurate contingency list with high redundancy could lead to intractable computational burdens and uneconomical solutions, while missing critical contingencies could render insecure solutions. In addition, the total time to calculate SCUC is always restricted

[21]. Thus, an efficient contingency selection method is desired to ensure computational efficiency and solution quality of the SCUC.

This paper is motivated by the needs of a more efficient and effective method for contingency selection in the context of SCUC problems. Specifically, different from the power flow based and PI based methods, this paper proposes an $N-1$ contingency selection method that simultaneously considers topological and physical vulnerabilities. Firstly, a power flow transferring path identification algorithm, which is developed based on the algorithm of k shortest paths and the concentric relaxation, is proposed to identify a set of transmission lines that may be overloaded after a line fails. Secondly, an index is proposed to access both topological and physical vulnerabilities of the identified lines and effectively rank contingencies. The most critical ones are then selected into a contingency list. Moreover, effectiveness of the proposed contingency selection method is verified in two steps. In the first step, the SCUC model is solved with the generated contingency list. In the second step, unit commitment and generation dispatch solutions from the SCUC model in the first step are evaluated against all $N-1$ contingencies, which calculate the total post-contingency generation-load imbalance against all $N-1$ contingencies.

The main contributions of this paper are two-fold:

1) The proposed method only uses topological structure and load information, which are naturally available in the SCUC problem. Instead of relying on power flow calculations, the power flow transferring path identification algorithm based on graph theory is used to identify the set of lines that may be overloaded after a transmission line fails. The proposed method can also accurately identify contingencies that cause system islanding and properly recognize their priorities in the contingency list.

2) Unlike the LODF based methods which usually derive the same LODF value for multiple contingencies and thus cannot rank contingencies properly, the proposed vulnerability index can effectively rank contingencies considering topological and physical characteristics of power grids. Moreover, the proposed method can generate dynamic contingency lists for multi-hour SCUC problems, which can derive more secure and economic SCUC solutions with respect to various operation conditions in different hours.

The remainder of this paper is organized as follows. Section II presents the proposed $N-1$ contingency selection method. Section III applies the generated contingency list to build the SCUC model, and discusses a full $N-1$ contingency security evaluation model to quantify security and economics of the corresponding SCUC solution. Section IV verifies the effectiveness of the proposed method via several benchmark IEEE test systems, and conclusions are drawn in Section V.

II. GRAPH THEORY BASED $N-1$ CONTINGENCY SELECTION

A. Topological Representation of Power Grids

1) Adjacency Matrix

According to graph theory, a power grid can be represent-

ed as a non-direction and non-weight graph $G(V,E)$ with sets of vertices and edges. The vertex set consists of buses, represented as $V=\{v_1, v_2, \dots, v_M\}$. The edge set consists of transmission lines, represented as $E=\{e_1, e_2, \dots, e_N\}$. The adjacency matrix of the graph $G(V,E)$, $A=(a_{ij})_{M \times M}$, is defined as in (1).

$$a_{ij} = \begin{cases} 0 & (i,j) \notin E \\ 1 & (i,j) \in E \end{cases} \quad (1)$$

In order to accurately reflect physical characteristics of the power grid, an enhanced weighted and directional adjacency matrix is further defined as in (2) by considering reactance and power flow directions of individual transmission lines.

$$a_{ij} = \begin{cases} 0 & (i,j) \notin E \\ \omega_{ij} & \text{power flow is from } i \text{ to } j, (i,j) \in E \\ -\omega_{ij} & \text{power flow is from } j \text{ to } i, (i,j) \in E \end{cases} \quad (2)$$

where ω_{ij} is the weight of transmission line (i, j) , which is set as its reactance in this paper.

2) Concentric Relaxation

Although failure of a transmission line will cause redistribution of power flows throughout the entire power system, it is well understood that the majority of power flow transfers through lines that are topologically close. A concept of tier is used to describe topological closeness of a line to the contingency [22]. Each tier consists of transmission lines that are directly connected to lines in the tier of one degree lower, i.e., tier T consists of lines that are directly connected to lines in tier $T-1$. As illustrated in Fig. 1, considering the contingency of line (i, j) , tier 1 consists of lines that are directly connected to line (i, j) , i.e., bus i and/or bus j , and tier 2 consists of lines that are directly connected to lines in tier 1.

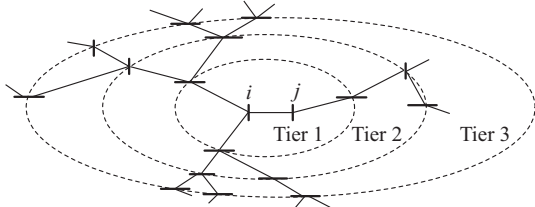


Fig. 1. Tiers in concentric relaxation.

According to the concept of concentric relaxation [23], [24], the impacts of a failure on lines in the tier 1 would be the most significant, and impacts would gradually reduce from tier 2 to tier 3. Moreover, a contingency may rarely cause overload for lines outside tier 3. As a result, instead of searching the whole power grid, transmission lines within the first three tiers of a contingency will be evaluated in this paper, so that the computational burden for large-scale power grids can be reduced. Moreover, in order to quantify the impacts of a contingency across multiple tiers, different weights are assigned to individual tiers, where inner tiers have higher weights indicating more significant impacts. That is, the concentric relaxation is used to refine the adjacency matrix constructed via (2). The weights of edges out-

side tiers 1-3 are set as 0, while the weights of edges in tiers 1, 2, and 3 are modified as $\pm 4\omega_{ij}/7$, $\pm 2\omega_{ij}/7$, and $\pm \omega_{ij}/7$, respectively.

B. Identification of Potential Overloaded Lines via Power Flow Transferring Path Identification Algorithm

1) Analysis on Power Flow Transferring Paths

Assuming that after a line fails, dispatches of generators and loads do not change right away, while the original power flow of this line will be redistributed to remaining lines in the system. Power flows of these remaining lines can be calculated by adding transferred power flows on top of the original ones. A power flow transferring path is defined as a set of lines that connect two ends of a disconnected line and transmit its originally carried power flow. Thus, by assessing power flow transferring paths, we would be able to identify lines that could be potentially overloaded after a line fails.

Figure 2 illustrates the power flow transferring process via a 9-bus system. Reactances of lines shown in Fig. 2 are per unit values. When line (1, 3) fails, it is replaced by an equivalent current source to calculate the transferred power flow as shown in Table I, where P_{ij} is the transferred power flow of line (i, j) . Figure 2 and Table I show that the most of the power flow of line (1, 3) is transferred to lines (1, 2) and (2, 3), which composes the shortest path between buses 1 and 3 (P1), followed by the second shortest path P2 and the third shortest path P3. P4 carries the smallest transferred power flow due to the longest path.

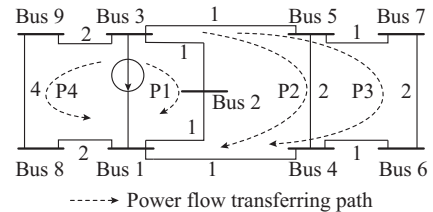


Fig. 2. Power flow transferring paths of a 9-bus system.

TABLE I
TRANSFERRED POWER FLOW OF EACH LINE IN A 9-BUS SYSTEM

Path	Reactance (p.u.)	Transferred power flow
P1: 1-2-3	2	$P_{12} = P_{23} = 0.5405P_{13}$
P2: 1-4-5-3	4	$P_{14} = P_{53} = 0.3243P_{13}$, $P_{45} = 0.2162P_{13}$
P3: 1-4-6-7-5-3	6	$P_{14} = P_{53} = 0.3243P_{13}$, $P_{46} = P_{67} = P_{75} = 0.1081P_{13}$
P4: 1-8-9-3	8	$P_{18} = P_{89} = P_{93} = 0.1351P_{13}$

This clearly shows that, when a transmission line fails, lines contained in the shortest path, i.e., with the smallest reactance, will have the largest transferred power flow, thus enduring higher overload possibilities. Therefore, by searching a few shortest paths between two vertices of a disconnected edge, we can identify potential overloaded transmission lines after an $N-1$ contingency occurs.

2) Identification of Potential Overloaded Transmission Lines

As discussed above, after the occurrence of a contingency, potential overloaded transmission lines could be identified

by searching the shortest paths. The general shortest path problem, which finds a path between two vertices in a non-direction graph with the smallest total edge weight, can be solved by Dijkstra's algorithm [25]. Moreover, the problem of k shortest paths [26], [27] can be solved via the extended Dijkstra's algorithm, with time complexity of $O(M + N \lg(N) + k)$.

The power flow transferring path identification algorithm is proposed to identify potential overloaded transmission lines after a contingency occurs. Firstly, the concentric relaxation is used to refine the adjacency matrix (2). In addition, the algorithm of k shortest paths is modified to identify all power flow transferring paths according to the refined adjacency matrix, instead of only k paths. In other words, power flow transferring paths within the three tiers are all identified. After power flow transferring paths are obtained, we identify the potential overloaded transmission lines by comparing power flow directions. If the original power flow direction of a line is consistent with the transferred power flow, the power flow of the line would increase, and overload may happen when the contingency occurs. Otherwise, power flow will decrease and overload may not occur. It is noteworthy that because topological neighbouring lines have comparable reactance and capacities, it is unlikely that transferred power flow will induce overload in the opposite direction.

The steps to identify potential overloaded transmission lines under a contingency is summarized in Algorithm 1. That is, for each contingency, Algorithm 1 is executed to obtain the list of potential overloaded transmission lines. It is noteworthy that information on original power flow directions used in Algorithm 1 is from SCUC power flows of the previous day.

Algorithm 1: identify potential overloaded transmission lines under a contingency

Input: weighted adjacency matrix from (2) and original power flow directions

- Step 1: refine the adjacency matrix (2) using the concentric relaxation
- Step 2: obtain power flow transferring paths via the power flow transferring path identification algorithm
- Step 3: identify potential overloaded transmission lines by comparing directions of original and transferred power flows

Output: potential overloaded transmission lines under the contingency

C. Vulnerability Index

In order to quantify severity of individual contingencies and rank them, the vulnerability index R^c is defined as in (3) according to the graph theory. In (3), topological betweenness $B_e(l)$ of line l , as defined in (4), is used to describe the vulnerability of an edge on connecting vertices [28]. However, by assuming weights of all edges to be 1, topological betweenness $B_e(l)$ neglects physical characteristics of the power grid, which may not accurately reflect vulnerabilities of lines. Thus, generalized load distribution factor (GLDF) $B_d(l)$ is also included in (3) to further represent physical characteristics of the power grid. GLDF is calculated as in (5) and (6).

$$R^c = \sum_{l \in \mathcal{K}^c} B_e(l) B_d(l) \quad (3)$$

$$B_e(l) = \sum_{i \in V} \sum_{j \in V} \frac{\sigma_{ij}(l)}{\sigma_{ij}} \quad (4)$$

$$B_d(l) = \sum_{d \in \mathcal{D}} D_{l,d} \frac{D_d}{\sum_{d'' \in \mathcal{D}} D_{d''}} \quad (5)$$

$$D_{l,d} = A_{l,d} + \frac{PL_l^b - \sum_{d' \in (\mathcal{D}-1)} A_{l,d'} D_{d'}}{\sum_{d'' \in \mathcal{D}} D_{d''}} \quad (6)$$

where \mathcal{K}^c is the set of potential overloaded transmission lines in contingency c ; σ_{ij} is the total number of the shortest paths between vertices i and j ; $\sigma_{ij}(l)$ is the number of the shortest paths between vertices i and j contain edge l ; \mathcal{D} is the set of loads; PL_l^b is the power flow of line l under normal operation condition; $A_{l,d}$ is the load shift distribution factor of load d on line l ; D_d is the electricity demand of load d ; $D_d / \sum_{d'' \in \mathcal{D}} D_{d''}$ is the weight of load d ; d' is the load not in the reference bus; and $D_{l,d}$ is the GLDF deduced from the generalized generation distribution factor (GGDF) [29]. That is, $D_{l,d}$ is the distribution coefficient of load d on transmission line l , representing the power flow component of line l delivered to load d .

In summary, $B_e(l)$ describes topological vulnerabilities of transmission line via betweenness, while $B_d(l)$ further represents physical vulnerabilities based on GLDF. Thus, the vulnerability index R^c , by accumulating vulnerabilities of all potential overloaded transmission lines, can reasonably quantify severity of contingencies. Because individual potential overloaded transmission lines have different $B_e(l)$, GLDF, $B_d(l)$, and \mathcal{K}^c under individual contingencies, values of R^c for individual contingencies will be different. Consequently, contingencies can be ranked easily based on R^c , where R^c of a larger value to an $N - 1$ contingency indicates a higher severity.

It is emphasized that R^c is calculated via static information. For a multi-time period problem such as multi-hour SCUC problem, distinct contingency lists can be used in different time periods to represent dynamic system characteristics. Thus, power flows and maximum power flow limits of lines can be added to further refine the vulnerability index R^c , as in (7), to derive a more accurate contingency selection process.

$$R^c = \sum_{l \in \mathcal{K}^c} B_e(l) B_d(l) \frac{PL_l^b}{PL_l^{\max}} \quad (7)$$

where PL_l^{\max} is the maximum power flow limit of line l .

D. Summary of $N - 1$ Contingency Selection Process

The proposed contingency selection process is summarized as follows:

- 1) Describe topology of the power grid and construct its adjacency matrix based on (2).
- 2) For each contingency, identify potential overloaded transmission lines using Algorithm 1.
- 3) Calculate the vulnerability index R^c of contingencies.
- 4) Rank contingencies based on vulnerability index R^c .

The generated contingency list will be used in the following section.

III. SCUC AND FULL $N-1$ CONTINGENCY SECURITY EVALUATION

As mentioned before, the $N-1$ contingency analysis includes two steps: contingency selection and contingency list evaluation. In this section, the effectiveness of the contingency list derived via the proposed contingency selection process is evaluated via SCUC. First, secure operation decisions are derived by solving the SCUC problem with the generated contingency list. Then, a full $N-1$ contingency security evaluation model is conducted to assess solution quality, thus illustrating the effectiveness of the derived contingency list.

A. SCUC Model Description

The objective of SCUC is to minimize the normal operation cost and post-contingency generation-load imbalance penalty cost as shown in (8).

$$\min \sum_{t \in \mathcal{T}} \left[\sum_{g \in \mathcal{G}} C_g^{\text{fuel}} \left(F_g^c(P_{g,t}^b) I_{g,t}^b + su_{g,t}^b + sd_{g,t}^b \right) + \sum_{e \in \mathcal{E}} \sum_{c \in \mathcal{C}} \text{VOLL} \cdot (v_{1,e,t}^c + v_{2,e,t}^c) \right] \quad (8)$$

where \mathcal{C} , \mathcal{E} , \mathcal{G} , and \mathcal{T} are the sets of contingency lists, buses, generators, and hours, respectively; $C_g^{\text{fuel}}(\cdot)$ is the fuel price of unit g ; $F_g^c(\cdot)$ is the heat rate curve of unit g ; $P_{g,t}^b$ is the generation dispatch of unit g at time t under normal operation condition; $I_{g,t}^b$ is the unit commitment status of unit g at time t under normal operation condition; $su_{g,t}^b$ and $sd_{g,t}^b$ are the start-up and shutdown costs of unit g at time t under normal operation condition, respectively; VOLL is the penalty cost of generation load imbalance; and $v_{1,e,t}^c$ and $v_{2,e,t}^c$ are the slack variables of load imbalance and generation imbalance of bus e at time t in contingency c , respectively.

The constraints for the normal operation condition are as follows:

$$P_g^{\min} I_{g,t}^b \leq P_{g,t}^b \leq P_g^{\max} I_{g,t}^b \quad g \in \mathcal{G}, t \in \mathcal{T} \quad (9)$$

$$P_{g,t}^b - P_{g,t-1}^b \leq UR_g \cdot I_{g,t-1}^b + P_g^{\min} (I_{g,t}^b - I_{g,t-1}^b) + P_g^{\max} (1 - I_{g,t}^b) \quad g \in \mathcal{G}, t \in \mathcal{T} \quad (10)$$

$$P_{g,t-1}^b - P_{g,t}^b \leq DR_g \cdot I_{g,t}^b + P_g^{\min} (I_{g,t-1}^b - I_{g,t}^b) + P_g^{\max} (1 - I_{g,t-1}^b) \quad g \in \mathcal{G}, t \in \mathcal{T} \quad (11)$$

$$(X_{g,t-1}^{\text{on}} - T_g^{\text{on}}) (I_{g,t-1}^b - I_{g,t}^b) \geq 0 \quad g \in \mathcal{G}, t \in \mathcal{T} \quad (12)$$

$$(X_{g,t-1}^{\text{off}} - T_g^{\text{off}}) (I_{g,t}^b - I_{g,t-1}^b) \geq 0 \quad g \in \mathcal{G}, t \in \mathcal{T} \quad (13)$$

$$\begin{cases} su_{g,t}^b \geq SU_g \cdot (I_{g,t}^b - I_{g,t-1}^b) \\ su_{g,t}^b \geq 0 \end{cases} \quad g \in \mathcal{G}, t \in \mathcal{T} \quad (14)$$

$$\begin{cases} sd_{g,t}^b \geq SD_g \cdot (I_{g,t-1}^b - I_{g,t}^b) \\ sd_{g,t}^b \geq 0 \end{cases} \quad g \in \mathcal{G}, t \in \mathcal{T} \quad (15)$$

$$\sum_{g \in N(e)} P_{g,t}^b - \sum_{s(l) \in N(e)} PL_{l,t}^b + \sum_{r(l) \in N(e)} PL_{l,t}^b = \sum_{d \in N(e)} P_{d,t} \quad e \in \mathcal{E}, g \in \mathcal{G}, l \in \mathcal{L}, t \in \mathcal{T} \quad (16)$$

$$-PL_l^{\max} \leq PL_{l,t}^b \leq PL_l^{\max} \quad l \in \mathcal{L}, t \in \mathcal{T} \quad (17)$$

$$PL_{l,t}^b = \frac{\theta_{s(l),t}^b - \theta_{r(l),t}^b}{x_l} \quad l \in \mathcal{L}, t \in \mathcal{T} \quad (18)$$

$$\begin{cases} \theta_e^{\min} \leq \theta_{e,t}^b \leq \theta_e^{\max} \\ \theta_{ref,t}^b = 0 \end{cases} \quad e \in \mathcal{E}, t \in \mathcal{T} \quad (19)$$

where P_g^{\min} and P_g^{\max} are the minimum and maximum capacities of unit g , respectively; UR_g and DR_g are the ramp-up and ramp-down rates of unit g , respectively; $X_{g,t-1}^{\text{on}}$ and $X_{g,t-1}^{\text{off}}$ are the on and off time counters of unit g at time $t-1$, respectively; T_g^{on} and T_g^{off} are the minimum on and off time limits of unit g , respectively; $PL_{l,t}^b$ is the power flow of line l at time t under normal operation condition; $s(l)$ and $r(l)$ are the sending and receiving buses of transmission line l , respectively; $N(e)$ is the set of network components connected at bus e ; SU_g and SD_g are the constant start-up and shutdown costs of unit g , respectively; $\theta_{s(l),t}^b$ and $\theta_{r(l),t}^b$ are the sending and receiving bus phase angles of line l at time t under normal operation condition, respectively; x_l is the reactance of transmission line l ; θ_e^{\min} and θ_e^{\max} are the minimum and maximum bus voltage phase angles of bus e , respectively; $\theta_{e,t}^b$ is the voltage phase angle of bus e at time t under normal operation condition; $\theta_{ref,t}^b$ is the voltage phase angle of the reference bus at time t under normal operation condition; and \mathcal{L} is the set of lines.

Constraints (9)-(15) describe operation limits for individual units. The power output of a generator is limited by its minimum and maximum capacities as in (9). Prevailing unit commitment constraints also include the ramp-up and ramp-down limits (10) and (11), the minimum on/off time limits (12) and (13), and the start-up and shutdown costs (14) and (15). Constraint (16) describes that the total power flow injection is equal to the total withdrawn at each node. Constraint (17) indicates that power flows of transmission lines need to meet capacity limits. In this paper, DC power flow model is used to calculate power flows of transmission lines according to line reactance and bus angles, as in (18) and (19).

The constraints under contingencies are as follows:

$$P_g^{\min} I_{g,t}^b \leq P_{g,t}^c \leq P_g^{\max} I_{g,t}^b \quad c \in \mathcal{C}, g \in \mathcal{G}, t \in \mathcal{T} \quad (20)$$

$$-R_g^{\text{down}} I_{g,t}^b \leq P_{g,t}^c - P_{g,t}^b \leq R_g^{\text{up}} I_{g,t}^b \quad c \in \mathcal{C}, g \in \mathcal{G}, t \in \mathcal{T} \quad (21)$$

$$\sum_{g \in N(e)} P_{g,t}^c - \sum_{s(l) \in N(e)} PL_{l,t}^c + \sum_{r(l) \in N(e)} PL_{l,t}^c + v_{1,e,t}^c - v_{2,e,t}^c = \sum_{d \in N(e)} P_{d,t} \quad c \in \mathcal{C}, e \in \mathcal{E}, g \in \mathcal{G}, l \in \mathcal{L}, t \in \mathcal{T} \quad (22)$$

$$\begin{cases} v_{1,e,t}^c \geq 0 \\ v_{2,e,t}^c \geq 0 \end{cases} \quad c \in \mathcal{C}, e \in \mathcal{E}, t \in \mathcal{T} \quad (23)$$

$$-PL_l^{\max} \leq PL_{l,t}^c \leq PL_l^{\max} \quad c \in \mathcal{C}, l \in \mathcal{L}, t \in \mathcal{T} \quad (24)$$

$$PL_{l,t}^c = \frac{\theta_{s(l),t}^c - \theta_{r(l),t}^c}{x_l} \quad c \in \mathcal{C}, l \in \mathcal{L}, t \in \mathcal{T} \quad (25)$$

$$\begin{cases} -\theta_e^{\max} \leq \theta_{e,t}^c \leq \theta_e^{\max} \\ \theta_{ref,t}^c = 0 \end{cases} \quad c \in \mathcal{C}, e \in \mathcal{E}, t \in \mathcal{T} \quad (26)$$

where $P_{g,t}^c$ is the generation dispatch of unit g at time t under contingency c ; R_g^{down} and R_g^{up} are the down and up corrective capabilities of unit g , respectively; $PL_{l,t}^c$ is the power flow of line l at time t under contingency c ; $\theta_{s(l),t}^c$ and $\theta_{r(l),t}^c$ are the sending and receiving bus voltage phase angles of line l at time t under contingency c , respectively; $\theta_{e,t}^c$ is the voltage phase angle of bus e at time t under contingency c ; and $\theta_{\text{ref},t}^c$ is the voltage phase angle of the reference bus at time t in contingency c .

Constraints (20)-(26) further ensure that the power system can operate securely after a single contingency occurs. Constraint (20) describes capacity limits of each unit, and constraint (21) indicates corrective capabilities of each unit. Compared with (16), slack variables are added in the nodal power balance equation (22) under contingencies, which allows load imbalance $v_{1,e,t}^c$ and/or generation imbalance $v_{2,e,t}^c$. Constraints (24)-(26) describe DC power flow constraints under each contingency.

B. Full $N - 1$ Contingency Security Evaluation

The SCUC problem (8)-(26) with different sets of contingencies derives different unit commitment and generation dispatch solutions under normal operation. These solutions, however, will induce diverse generation-load imbalance performance under other $N - 1$ contingencies outside the contingency list used in SCUC. To this end, a full $N - 1$ contingency security evaluation model is proposed to assess quality of the SCUC solution in terms of the total generation-load imbalance under all $N - 1$ contingencies, thereby evaluating the effectiveness of the generated contingency lists.

The objective of the full $N - 1$ contingency security evaluation problem is to minimize the generation-load imbalance under all $N - 1$ contingencies as in (27), with respect to the unit commitment and generation dispatch solutions for the normal condition. The constraints include (16)-(26) that are implemented on all $N - 1$ contingencies, namely $c \in \mathcal{C}'$.

$$\min \sum_{e \in \mathcal{C}} \sum_{c \in \mathcal{C}'} \sum_{t \in T} (v_{1,e,t}^c + v_{2,e,t}^c) \tag{27}$$

A smaller objective means less generation-load imbalance against all contingencies, indicating a better SCUC solution that benefits from the more effective contingency list.

IV. NUMERICAL EXAMPLE

The IEEE 5-bus, 24-bus, and 118-bus systems are used to evaluate the effectiveness of proposed method in selecting and evaluating contingencies. The IEEE 5-bus system is used first to show advantages of the proposed method in identifying potential overloaded transmission lines under contingency and in ranking contingencies. The IEEE 24-bus system is used to illustrate the performance of the proposed method in identifying contingencies that cause system islanding. The IEEE 118-bus system finally shows the application of the proposed method on large-scale power grids. All numerical examples are carried out on a personal computer with Intel Core i7 3.20 GHz processor and 16 GB memory.

A. IEEE 5-bus System

The IEEE 5-bus system in Fig. 3 includes 5 buses and 6

branches. Using the power flow transferring path identification algorithm, potential overloaded transmission lines are identified, as shown in Table II. Vulnerability index R^c is also calculated according to (3) to rank contingencies. The total computation time is 0.0036 s. The LODF method [11], [30] is also included in Table III for comparison.

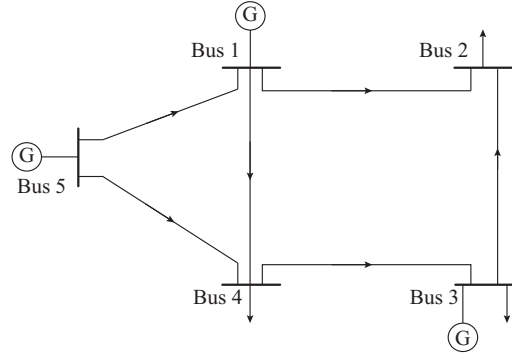


Fig. 3. Topology of IEEE 5-bus system.

TABLE II
CONTINGENCY RANK OF IEEE 5-BUS SYSTEM

Contingency line ID	Potential overloaded transmission line	R^c	Rank of R^c
1-2	1-4, 2-3, 3-4, 4-5	0.5690	1
1-4	1-2, 4-5	0.3183	6
1-5	2-3, 3-4, 4-5	0.4356	3
2-3	1-2, 1-5	0.3791	4
3-4	1-2, 1-5	0.3791	4
4-5	1-2, 1-4, 1-5	0.5126	2

Table III shows the LODFs of each transmission line on other transmission lines.

TABLE III
LODFs OF IEEE 5-BUS SYSTEM

ID of outage transmission line	LODF of other transmission lines					
	1-2	1-4	1-5	2-3	3-4	4-5
1-2	0	-0.5429	-0.4571	1.0000	1.0000	0.4571
1-4	-0.3448	0	-0.6552	-0.3448	-0.3448	0.6552
1-5	-0.3071	-0.6929	0	-0.3071	-0.3071	-1.0000
2-3	1.0000	-0.5429	-0.4571	0	1.0000	0.4571
3-4	1.0000	-0.5429	-0.4571	1.0000	0	0.4571
4-5	0.3071	0.6929	-1.0000	0.3071	0.3071	0

According to the method in [11], a larger absolute LODF value indicates that the outage of this transmission line will have more severe impacts on other transmission lines, thus it will have a higher priority to be added in the contingency list. For the IEEE 5-bus system, five transmission lines, except line 1-4, will be selected because of their ± 1 LODF values on other transmission lines. However, these five identified contingencies cannot be properly ranked because they all have the same absolute LODF value of 1. Moreover, under a certain contingency, some transmission lines with large absolute LODF values may not be overloaded. For instance,

lines 2-3 and 3-4 have LODF values of 1 on each other, which means if line 2-3 is on outage, the power flow redistributed to line 3-4 will be equal to the original power flow of line 2-3. However, as the redistributed power is in opposite direction of the original power flow of line 3-4, the actual power flow would decrease and overload may not happen.

In comparison, as shown in Table II, potential overloaded transmission lines identified by the proposed method may not necessarily have the largest absolute LODF values. However, they are transmission lines whose power flows will increase under contingencies. In addition, the vulnerability index can effectively rank severity of contingencies, thus contingencies with larger R^c can be added to the contingency list for the usage of power system applications.

B. IEEE 24-bus System

1) Contingency Selection for Static SCUC

The IEEE 24-bus system in Fig. 4 includes 24 buses and 38 branches. To facilitate our studies, capacity limits of all transmission lines are reduced to 75% of their original values. The power flow transferring path identification algorithm and the vulnerability index are used first to select contingencies, with the total computation time of 0.7291 s. The LODF method and power flow method are also included for comparison. The main idea of the power flow method is to use DC power flow calculation to identify contingencies that would cause overload of other transmission lines under the normal operation condition. Here, size of the contingency list is set to 15 for fair comparison among the three methods, because the LODF method identifies 14 contingencies, which are all with the largest absolute LODF values of 1 and cannot be properly ranked.

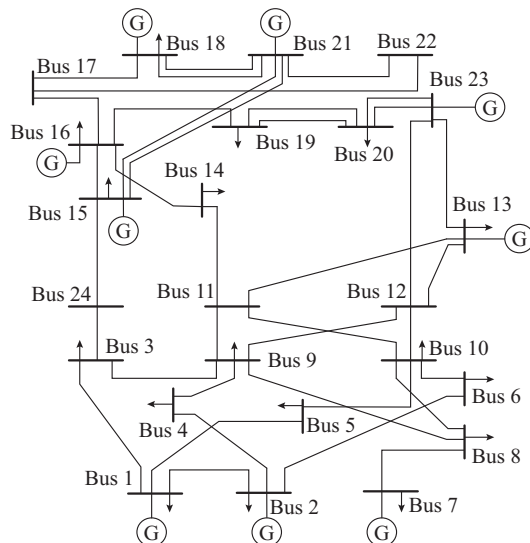


Fig. 4. Topology of IEEE 24-bus system.

Contingency lists identified via the LODF method and the proposed method are compared in Table IV. As contingency lists from the power flow method are different in different hours, they are not included here due to space limit. Transmission lines 20-23(1) and 20-23(2) are parallel lines that constitute the corridor between bus 20 and bus 23, which

are both critical ones and included in the contingency list according to the proposed method. In this system, the contingency of transmission line 7-8 disconnects bus 7 and bus 8, islanding generator and load at bus 7 from the rest of the system, which could potentially result in large generation-load imbalance.

TABLE IV
CONTINGENCY LIST OF IEEE 24-BUS SYSTEM

Contingency transmission selection method	Contingency list
LODF	1-5, 2-4, 2-6, 3-24, 4-9, 5-10, 6-10, 8-9, 8-10, 11-14, 14-16, 15-24, 17-22, 21-22, 16-17
Proposed method	1-5, 2-6, 3-9, 3-24, 4-9, 7-8, 8-9, 9-11, 11-13, 11-14, 13-23, 14-16, 15-24, 20-23(1), 20-23(2)
LODF + islanding contingencies	1-5, 2-4, 2-6, 3-24, 4-9, 5-10, 6-10, 8-9, 8-10, 11-14, 14-16, 15-24, 17-22, 21-22, 7-8

Table IV clearly shows that the proposed power flow transferring path identification algorithm can effectively identify contingencies that cause system islanding. Specifically, it is shown that transmission line 7-8 is included in the list from the proposed method, while the list from the LODF method only contains contingencies with larger absolute LODF values. To this end, we have to manually add transmission line 7-8 to the list of the LODF method to form contingency list from LODF + islanding contingencies method, which, however, may not be achievable for systems with large scales and complicated topologies.

In order to further evaluate the effectiveness of the contingency lists identified via the above three methods, the 24-hour SCUC models with respect to the three contingency lists are first solved to derive secure and economic operation decisions, which are then evaluated via the full $N-1$ security evaluation process (with a total of 38 $N-1$ contingences for the IEEE 24-bus system). Results of SCUC and full $N-1$ security evaluation are shown in Table V.

TABLE V
SCUC AND FULL $N-1$ SECURITY EVALUATION RESULTS OF IEEE 24-BUS SYSTEM

Contingency selection method	SCUC objective (\$)	Full $N-1$ security evaluation		
		Objective (MW)	Load imbalance (MW)	Generation imbalance (MW)
LODF	2607825.94	1320.42	909.00	411.42
LODF + islanding contingencies	2616699.63	360.32	360.32	0
Power flow	2612760.24	925.34	501.71	423.63
Power flow + islanding contingencies	2619552.10	34.50	34.50	0
Proposed method	2616486.16	34.36	34.36	0

As shown in Table V, although the proposed method derives the largest normal operation cost by accurately including critical contingencies, it has the smallest generation-load imbalance in the full $N-1$ security evaluation, i.e., the most

secure SCUC solution. Specifically, generation imbalance of the proposed method is 0, because the proposed method can effectively identify critical contingencies leading to system islanding. In comparison, the LODF method cannot correctly identify those contingencies due to their 0 LODF values on other transmission lines. Similarly, because the occurrence of a system islanding contingency will not cause changes of power flows for remaining lines according to the DC power flow calculation, the power flow method will not effectively identify those system islanding contingencies as high priority ones.

For further comparison, we manually add transmission line 7-8 to contingency lists of LODF method and power flow method to obtain new SCUC decisions and full $N-1$ security evaluation results, as shown in Table V. By further considering this specific islanding contingency, the SCUC objectives increase with zero generation imbalance and decrease with load imbalance. However, compared with the new LODF method based SCUC result with the islanding contingency, the proposed method still has a better performance in terms of a smaller load imbalance. This is because the proposed method can accurately identify potential overloaded transmission lines via power flow transferring path identification algorithm, while some transmission lines with large LODF values identified by the LODF method may not actually overload, as analysed in Section IV-A. In addition, the new power flow method based SCUC result also improves by adding contingency line 7-8. Indeed, it derives similar load imbalance level as the proposed method. However, its normal operation costs in the SCUC solution is larger than the proposed method. In summary, the proposed method has a better performance than the LODF method and the power flow method, by effectively identifying islanding contingencies and accurately assessing potential overloaded transmission lines in the contingency selection process to derive more secure and economic SCUC solutions.

2) Contingency Selection for Dynamic SCUC

The dynamic contingency selection for the IEEE 24-bus system is further carried out to evaluate if such time-dependent dynamic contingency lists could help derive better SCUC decision. Specifically, by using more information, the vulnerability index is updated for each hour according to (7). The total computation time is 15.5588 s. For the sake of fair comparison, power flow information is also added to improve the LODF method [11], while the size of the contingency list is determined by a prespecified threshold value.

The results of SCUC and full $N-1$ security evaluation are shown in Table VI, by setting size of the hourly contingency list of the proposed method to 3-10, respectively. Table VII further shows the results of the improved LODF method by setting the threshold value to be 0.60, 0.55, 0.50, 0.45, 0.40, and 0.35, respectively. The results of the improved LODF method while manually adding islanding contingency line 7-8 are also included.

TABLE VI
DYNAMIC SCUC AND FULL $N-1$ SECURITY EVALUATION RESULTS OF PROPOSED METHOD FOR IEEE 24-BUS SYSTEM

Length of contingency list	SCUC objective (\$)	Full $N-1$ security evaluation		
		Objective (MW)	Load imbalance (MW)	Generation imbalance (MW)
3	2608951.84	332.27	332.27	0
4	2609651.23	320.44	320.44	0
5	2612734.09	34.50	34.50	0
6	2612734.09	34.50	34.50	0
7	2613132.76	34.36	34.36	0
8	2613132.76	34.36	34.36	0
9	2613132.76	34.36	34.36	0
10	2616486.16	34.36	34.36	0

TABLE VII
DYNAMIC SCUC AND FULL $N-1$ SECURITY EVALUATION RESULTS OF IMPROVED LODF METHOD FOR IEEE 24-BUS SYSTEM

Threshold value	Improved LODF				Improved LODF + islanding contingencies			
	Average length of contingency list	SCUC objective (\$)	Full $N-1$ security evaluation		Average length of contingency list	SCUC objective (\$)	Full $N-1$ security evaluation	
			Load imbalance (MW)	Generation imbalance (MW)			Load imbalance (MW)	Generation imbalance (MW)
0.60	4.75	2604461.49	888.90	411.42	5.75	2612703.92	332.13	0
0.55	5.05	2604461.49	888.90	411.42	6.05	2612703.92	332.13	0
0.50	5.50	2604461.49	888.90	411.42	6.50	2612703.92	332.13	0
0.45	5.88	2604461.49	888.90	411.42	6.88	2612703.92	332.13	0
0.40	6.71	2604750.49	800.43	411.42	7.71	2613003.27	220.30	0
0.35	8.33	2609395.79	481.62	423.63	9.33	2616486.16	34.36	0

The proposed dynamic contingency selection method has a better performance than both the improved LODF method and the improved LODF + islanding contingencies. Specifically, with the size of hourly contingency list being 7, the proposed method achieves the smallest load imbalance 34.36 MW with the normal operation SCUC cost of \$2613132.76. However, to achieve the same level of load imbalance, the improved LODF method derives a higher normal operation

cost of \$2616486.16 with average size of hourly contingency list of 9.33. It clearly shows that the proposed method could identify severe contingencies efficiently and accurately, which also derives more economical SCUC solutions at the similar security level.

More importantly, the proposed method could accurately identify critical contingencies to derive secure SCUC solutions more effectively, in terms of less total generation-load

imbalance for all $N-1$ contingencies. Indeed, for the IEEE 24-bus system, the most secure SCUC solution will still result in 24.21 MW generation-load imbalance, due to adjustments on transmission line capacity limits. That is, the IEEE 24-bus system has at least a generation-load imbalance of 24.21 MW with respect to all $N-1$ contingencies, even all 38 $N-1$ contingencies are considered to determine the most secure SCUC decision. With the size of 13 contingencies, the proposed method can obtain the smallest generation-load imbalance level, which cannot be achieved by the improved LODF method and the improved LODF + islanding contingencies under similar contingency list size.

C. IEEE 118-bus System

The IEEE 118-bus system including 118 buses and 184 branches is used to evaluate effectiveness of the proposed method on large-scale power grids. For large-scale power systems, concentric relaxation can effectively mitigate computational burden in terms of the number of nodes and edges to be searched by the power flow transferring path identification algorithm. Taking contingency of transmission line 4-5 as an example, the nodes and edges searched in power flow transferring path identification algorithm are 21 and 23, respectively. The computation time on contingency selection in static SCUC and dynamic SCUC are 75.6632 s and 286.2671 s, respectively, which shows the potential of the proposed method for online applications of large-scale power grids.

The SCUC results with static and dynamic contingency lists and their corresponding full $N-1$ security evaluation results are shown in Table VIII.

TABLE VIII
SCUC RESULTS WITH STATIC AND DYNAMIC CONTINGENCY LISTS AND CORRESPONDING FULL $N-1$ SECURITY EVALUATION RESULTS

Length of contingency list	With static contingency list		With dynamic contingency list	
	SCUC result (\$)	Full $N-1$ security evaluation result (MW)	SCUC result (\$)	Full $N-1$ security evaluation result (MW)
20	17354103.26	7326.50	15176119.77	5672.10
21	17348207.57	6558.52	15178259.31	5669.34
22	17348207.57	6558.52	15178989.88	5626.19
23	17363132.90	6421.23	15179545.60	5603.45
24	17403524.11	6394.77	15179612.63	5565.77
25	17403524.11	6394.77	15181337.94	5550.26

As shown in Table VIII, for both static and dynamic cases, the normal operation cost increases with increase in the size of contingency list, while also enhancing the security of the power grid with reduced generation-load imbalance. On the other hand, by leveraging more information to calculate vulnerability index, the dynamic contingency list could identify critical contingencies more accurately over the time. Thus, with contingency list of the same size, SCUC results with the dynamic contingency list presents a better performance in terms of smaller normal operation cost and lower

generation-load imbalance in the full $N-1$ security evaluation.

V. CONCLUSION

Efficient and accurate contingency selection approaches play an important role in designing secure and economic operation strategies of power grids. By analysing limitations of state-of-the-art contingency selection methods, this paper discusses a novel graph theory based $N-1$ contingency selection method for SCUC problem. The full $N-1$ security evaluation model is further adopted to assess the quality of SCUC solutions, thus illustrating effectiveness of the derived contingency list. Numerical results on IEEE benchmark systems show several advantages of the proposed contingency selection method:

1) The proposed power flow transferring path identification algorithm can effectively identify contingencies that cause system islanding conditions.

2) The vulnerability index R can effectively rank contingencies and consequently help identify the critical ones with the highest priorities.

3) The proposed contingency selection approach can also help derive dynamic contingency lists according to distinct system status at different time periods, and can thus derive more secure and economic SCUC solutions than that from the static contingency list.

4) Because of its high computational performance, the proposed method could be potentially used for online applications such as security assessment and special protection system implementation.

5) Future work could investigate the impacts of load and renewable generation uncertainties on the contingency selection as well as the SCUC solutions.

REFERENCES

- [1] K. W. Hedman, M. C. Ferris, R. P. O'Neill *et al.*, "Co-optimization of generation unit commitment and transmission switching with $N-1$ reliability," *IEEE Transactions on Power Systems*, vol. 25, no. 2, pp. 1052-1063, May 2010.
- [2] M. Khanabadi, H. Ghasemi, and M. Doostizadeh, "Optimal transmission switching considering voltage security and $N-1$ contingency analysis," *IEEE Transactions on Power Systems*, vol. 28, no. 1, pp. 542-550, Feb. 2013.
- [3] N. Fan, H. Xu, F. Pan *et al.*, "Economic analysis of the $N-k$ power grid contingency selection and evaluation by graph algorithms and interdiction methods," *Energy Systems*, vol. 2, no. 3, pp. 313-324, Nov. 2011.
- [4] Z. Li, J. Wang, H. Sun *et al.*, "Transmission contingency analysis based on integrated transmission and distribution power flow in smart grid," *IEEE Transactions on Power Systems*, vol. 30, no. 6, pp. 3356-3367, Nov. 2015.
- [5] Z. Li, J. Wang, H. Sun *et al.*, "Transmission contingency screening considering impacts of distribution grids," *IEEE Transactions on Power Systems*, vol. 31, no. 2, pp. 1659-1660, Mar. 2016.
- [6] M. Sahraei-Ardakani, X. Li, P. Balasubramanian *et al.*, "Real-time contingency analysis with transmission switching on real power system data," *IEEE Transactions on Power Systems*, vol. 31, no. 3, pp. 2501-2502, May 2016.
- [7] Y. Zhao, C. Yuan, G. Liu *et al.*, "Graph-based preconditioning conjugate gradient algorithm for " $N-1$ " contingency analysis," in *Proceedings of 2018 IEEE PES General Meeting*, Portland, USA, Aug. 2018, pp. 1-5.
- [8] M. Wang, M. Yang, J. Wang *et al.*, "Contingency analysis considering the transient thermal behavior of overhead transmission lines," *IEEE*

- Transactions on Power Systems*, vol. 33, no. 5, pp. 4982-4993, Sept. 2018.
- [9] A. M. Al-Shaalan, "Contingency selection and ranking for composite power system reliability evaluation," *Journal of King Saud University-Engineering Sciences*, vol. 32, no. 2, pp. 141-147, Nov. 2018.
- [10] P. Mitra, V. Vittal, B. Keel *et al.*, "A systematic approach to $n-1-1$ analysis for power system security assessment," *IEEE Power and Energy Technology Systems Journal*, vol. 3, no. 2, pp. 71-80, Jun. 2016.
- [11] C. M. Davis and T. J. Overbye, "Multiple element contingency screening," *IEEE Transactions on Power Systems*, vol. 26, no. 3, pp. 1294-1301, Aug. 2011.
- [12] P. Kaplunovich and K. Turitsyn, "Fast and reliable screening of $N-2$ contingencies," *IEEE Transactions on Power Systems*, vol. 31, no. 6, pp. 4243-4252, Nov. 2016.
- [13] T. Y. Hsiao, C. A. Hsieh, and Chan-Nan Lu, "A risk-based contingency selection method for SPS applications," *IEEE Transactions on Power Systems*, vol. 21, no. 2, pp. 1009-1010, May 2006.
- [14] N. Amjadi and M. Esmaili, "Application of a new sensitivity analysis framework for voltage contingency ranking," *IEEE Transactions on Power Systems*, vol. 20, no. 2, pp. 973-983, May 2005.
- [15] D. Liu, C. K. Tse, and X. Zhang, "Robustness assessment and enhancement of power grids from a complex network's perspective using decision trees," *IEEE Transactions on Circuits and Systems II: Express Briefs*, vol. 66, no. 5, pp. 833-837, May 2019.
- [16] L. Nan, T. Liu, and C. He, "Identification of transmission sections based on power grid partitioning," *International Transactions on Electrical Energy Systems*, vol. 29, no. 2, pp. 2793, Dec. 2018.
- [17] E. P. R. Coelho, M. H. M. Paiva, M. E. V. Segatto *et al.*, "A new approach for contingency analysis based on centrality measures," *IEEE Systems Journal*, vol. 13, no. 2, pp. 1915-1923, Jun. 2019.
- [18] G. A. Pagani and M. Aiello, "The power grid as a complex network: a survey," *Physica A: Statistical Mechanics and Its Applications*, vol. 392, no. 11, pp. 2688-2700, Jun. 2013.
- [19] G. Irisarri, D. Levner, and A. M. Sasson, "Automatic contingency selection for on-line security analysis—real-time tests," *IEEE Transactions on Power Apparatus and Systems*, vol. PAS-98, no. 5, pp. 1552-1559, Sept. 1979.
- [20] G. D. Irisarri and A. M. Sasson, "An automatic contingency selection method for on-line security analysis," *IEEE Transactions on Power Apparatus and Systems*, vol. PAS-100, no. 4, pp. 1838-1844, Apr. 1981.
- [21] NYISO. (2013, Jun.). Market participants user's guide. [Online]. Available: <https://www.nyiso.com/documents/20142/3625950/mpug.pdf>
- [22] L. Wu, G. K. Venayagamoorthy, R. G. Harley *et al.*, "Cellular computational networks based voltage contingency ranking regarding power system security," in *Proceedings of 2018 Clemson University Power Systems Conference (PSC)*, Charleston, USA, Sept. 2018, pp. 1-8.
- [23] J. Zaborszky, K. Whang, and K. Prasad, "Fast contingency evaluation using concentric relaxation," *IEEE Transactions on Power Apparatus and Systems*, vol. PAS-99, no. 1, pp. 28-36, Jan. 1980.
- [24] A. J. Wood and B. F. Wollenberg, *Power Generation, Operation, and Control*, New York: John Wiley & Sons, pp. 97-108, 2012.
- [25] E. W. Dijkstra, "A note on two problems in connexion with graphs," *Numerische Mathematik*, vol. 1, no. 1, pp. 269-271, Jan. 1959.
- [26] D. Eppstein, "Finding the K shortest paths," *SIAM Journal on Computing*, vol. 28, no. 2, pp. 652-673, May 1998.
- [27] Y. Yamane and H. Kitajima. (2019, Aug.). A new k -shortest path search approach based on graph reduction. [Online]. Available: <https://arxiv.org/abs/1908.06460v1>
- [28] M. E. J. Newman, "A measure of betweenness centrality based on random walks," *Society Networks*, vol. 27, no. 1, pp. 39-54, Jan. 2005.
- [29] W. Y. Ng, "Generalized generation distribution factors for power system security evaluations," *IEEE Power Engineering Review*, vol. PER-1, no. 3, pp. 18-19, Mar. 1981.
- [30] J. Guo, Y. Fu, Z. Li *et al.*, "Direct calculation of line outage distribution factors," *IEEE Transactions on Power Systems*, vol. 24, no. 3, pp. 1633-1634, Aug. 2009.

Lu Nan received the B.S. and the Ph.D. degrees in electrical engineering from Sichuan University, Chengdu, China, in 2016 and 2020, respectively. Currently, she is a research associate in College of Electrical Engineering, Sichuan University. She was a visiting Ph.D. student at Stevens Institute of Technology, Hoboken, USA, from 2018 to 2019. Her research interests include vulnerability analysis and optimal operation of power grids.

Yikui Liu received the B.S. degree in electrical engineering and automation from Nanjing Institute of Technology, Nanjing, China, in 2012, and the M. S. degree in power system and automation from Sichuan University, Chengdu, China, in 2015. He is currently pursuing the Ph.D. degree with Electrical and Computer Engineering Department, Stevens Institute of Technology, Hoboken, USA. His current research interests are power market and optimal power flow in distribution system.

Lei Wu received the B.S. degree in electrical engineering and the M.S. degree in systems engineering from Xi'an Jiaotong University, Xi'an, China, in 2001 and 2004, respectively, and the Ph.D. degree in electrical engineering from the Illinois Institute of Technology (IIT), Chicago, USA, in 2008. He was a senior research associate with the Robert W. Galvin Center for Electricity Innovation, IIT from 2008 to 2010. He worked as summer visiting faculty at NYISO in 2012. He was a professor with the Electrical and Computer Engineering Department, Clarkson University, Potsdam, USA till 2018. Currently, he is an Associate Professor with the Electrical and Computer Engineering Department, Stevens Institute of Technology, Hoboken, USA. His research interests include power systems operation and planning, energy economics, and community resilience microgrid.

Tianqi Liu received the B.S. and the M.S. degrees from Sichuan University, Chengdu, China, in 1982 and 1986, respectively, and the Ph.D. degree from Chongqing University, Chongqing, China, in 1996, all in electrical engineering. Currently, she is a professor in College of Electrical Engineering, Sichuan University. Her main research interests include power system analysis and stability control, HVDC, optimal operation, dynamic security analysis, dynamic state estimation and load forecasting.

Chuan He received the B.S., M.S., and the Ph.D. degrees in electrical engineering from Sichuan University, Chengdu, China, in 2011, 2014, and 2018, respectively. Currently, he is an Associate Professor in College of Electrical Engineering, Sichuan University. He was a visiting Ph.D. student at Clarkson University, Potsdam, USA, from 2015 to 2017. His research interests include robust optimization on power system operation and planning with renewable energy.